Electronically scanned antenna arrays made of advanced materials

M. G. ȚURCAN*, I. NICOLAESCU
Military Technical Academy „Ferdinand I", Faculty of Communications and Electronics Systems for Defence and Security, 39-49 George Coșbuc Blvd., 050141, Bucharest, Romania

A 1 × 4 cylindrical dielectric resonator antenna array with a steerable beam pattern is designed, fabricated and presented in this paper. The cylindrical dielectric resonator antennas, with a dielectric constant of 34, are excited using aperture coupling and are operated at the fundamental $HE_{11\delta}$ mode. Four PIN diode phase shifters, printed on the same Rogers 4003 substrate, with a dielectric constant of 3.55, are used to steer the main beam on three directions, at 5.2 GHz. The maximum steering angle obtained was ± 36 degree. A practical model has been implemented. The practical results are similar to the simulation results.

(Received July 10, 2023; accepted August 10, 2023)

Keywords: Microstrip phase shifter, PIN diode, Steering angle, Main beam, Cylindrical dielectric resonator antenna array

1. Introduction

Space communications, military radar, Wi-Fi and LTE technology, or health care applications require electronically steerable beam patterns, which can be achieved using phased array antennas.

The antenna array beam can be steered in a desired direction by changing the phase of each element of the array [1]. This can be achieved by feeding each element of the array through a phase shifter.

The phase shifter structure can be electronically controlled by using PIN diodes as switching devices [2]. The switching procedure of a PIN diode can be performed by changing the bias from forward to reverse and vice-versa.

A bias circuit model for the PIN diode is presented in this article, to supply the specific bias voltage and current. To simplify the bias circuit manufacture process, the electronic components, such as inductors and capacitors, will be replaced by microstrip lines.

In this paper, a 1 × 4 cylindrical dielectric resonator antenna array, at 5.2 GHz, is designed. PIN diodes from Infineon were used in the construction of the phase shifters, such as: BAR50-02V, BAR64-02V, BAR64-02EL, BAR90-02EL and BAR90-02ELS. For each individual case, the antenna array parameters were simulated and analyzed using the High Frequency Structural Simulator (HFSS) from Ansys.

2. Experimental

The geometric configuration of the 1 × 4 cylindrical dielectric resonator antenna (CDRA) array is shown in Fig. 1.

Four CDRA are located on a Rogers 4003 grounded substrate, of length 86 mm and width 158 mm, with dielectric constant ε_s = 3.55 and thickness t = 0.813 mm. The elements are separated by $\lambda_0/2$, where λ_0 is the free-space wavelength at the resonant frequency.

According to [3-4], the resonance frequency of resonators, with dielectric constant ε_r = 34, radius a = 4.55 mm and height h = 3.7 mm, is 5.51 GHz.

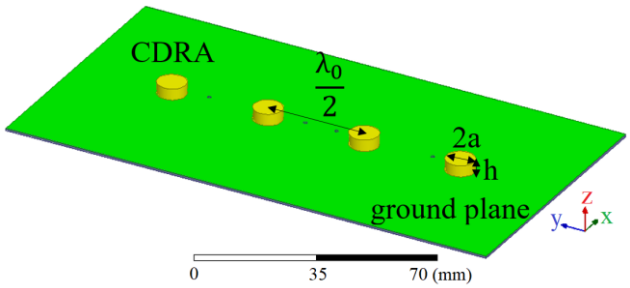

Fig. 1. 1 × 4 CDRA array geometry – top view (color online)

Four apertures, having dimensions l_s = 3 mm and w_s = 2 mm, will excite the fundamental $HE_{11\delta}$ modes of the CDRAs.

The CDRAs, with dielectric constant ε_r = 34, radius a = 4.55 mm and height h = 3.7 mm, are centered over the apertures, to ensure strong coupling to the internal magnetic fields.

The PIN diode phase shifter electric circuit is shown in Fig. 2.

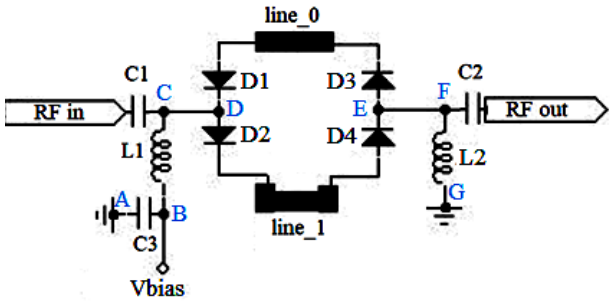

Fig. 2. PIN diode phase shifter electric circuit (color online)

The design of a phase shifter shows two transmission lines of different lengths. Each of the traces can be switched to provide different phase shifts. A gap of 0.4 mm is placed between the transmission lines. A PIN diode switch will be placed in each gap in order to extend the transmission line.

The differential phase shift between two transmission lines (l_1 and l_0) is given by the following equation [5]:

$$\Delta\phi = \beta \times (l_1 - l_0) \tag{1}$$

where, β is propagation constant of the transmission line and ε_{eff} is effective microstrip permittivity:

$$\beta = \frac{2\pi}{\lambda_0}\sqrt{\varepsilon_{eff}} \tag{2}$$

The differences between the physical lengths of the delay lines and the reference line (l_0), are presented in Table 1.

Table 1. The differences between the lengths of two transmission lines

No.	ΔØ	ΔL	Length
1	120°	l_1-l_0	11.54 mm
2	240°	l_2-l_0	23.08 mm

Capacitors C1 and C2 are to provide RF connectivity and block direct current (DC) signals, while inductors L1 and L2 are designed to suppress the high-frequency alternating current (AC) signals, and to allow the circulation of DC signals.

If C1 = C2 = 100 pF, the corresponding impedance at the operating frequency f_0 = 5.2 GHz, is small enough so it doesn't affect the 50 Ω impedance of the circuit ($Zc_1 = Zc_2$ =0.30 Ω).

If L1 = L2 = 7.6 nH, the corresponding impedance at the operating frequency, f_0 = 5.2 GHz, is high enough so it doesn't interfere with the circuit ($Z_{L1} = Z_{L2}$ = 248 Ω).

The bias circuit manufacturing process is simplified by replacing the electronic components, such as inductors and capacitors, with microstrip lines.

The length of the microstrip line that behaves as an inductor/capacitor is derived from [6]:

$$l_i = \frac{\lambda}{2\pi}\left[n\pi + arctg\left(\frac{\omega L}{Z_0}\right)\right], n \in N \tag{3}$$

$$l_c = \frac{\lambda}{2\pi}\left[(n+1)\pi - arctg\left(\frac{1}{\omega C Z_0}\right)\right], n \in N \tag{4}$$

where, λ is the wavelength and Z_0 is the characteristic impedance of the transmission line, which is calculated with the formula from [7].

The phase shifter bias circuit can be bulky so, in order to reduce the size of the matching network, radial stubs can be used.

Fig. 3 (a) shows the radial stub versus the conventional open stub. The equivalent capacitance value, at the frequency f_0 = 5.2 GHz, is the same for both transmission lines. The proposed shape length (according to [8]) represents 30% of the conventional shape length, making the matching network more compact.

The proposed phase shifter model is shown in Fig. 3 (b). The CB and FG microstrip lines with a width of 0.1 mm and a length of λ/4 are the inductors L1 and L2 from Fig. 2. The radial stub AB is the capacitor C3.

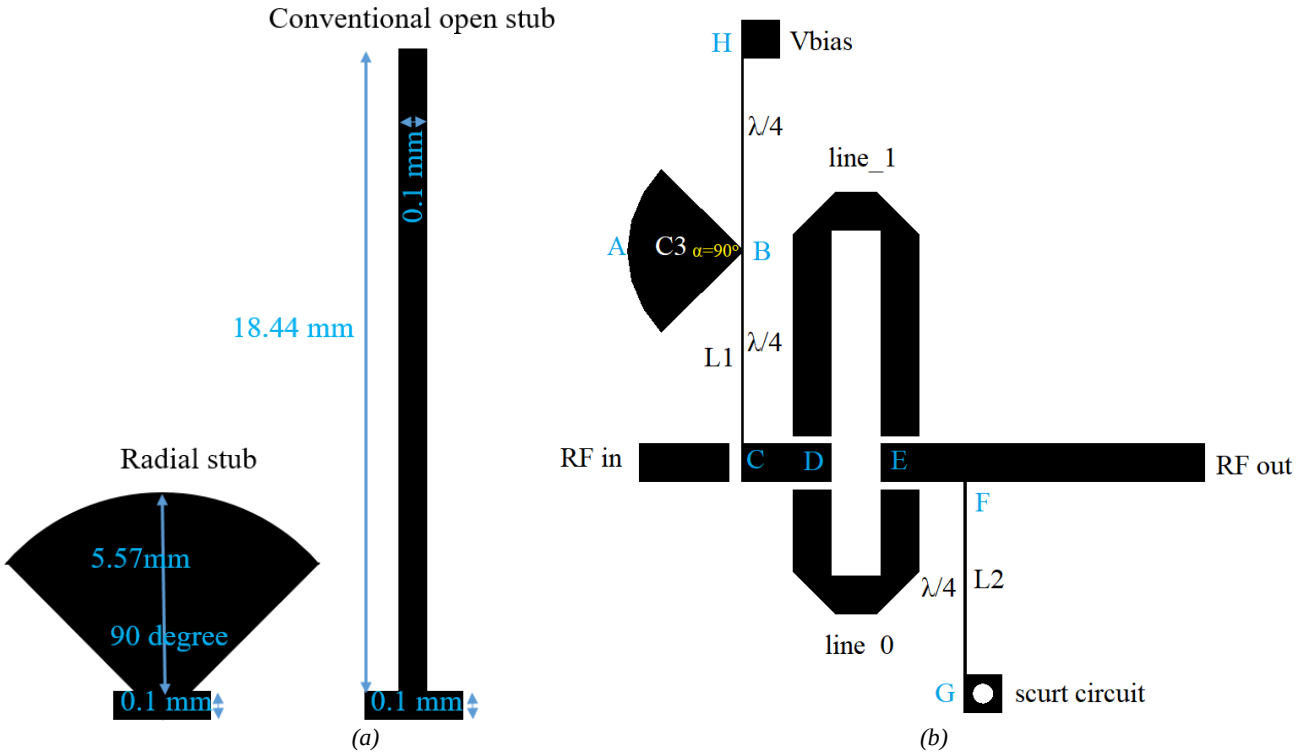

Fig. 3. (a) Radial stub versus conventional open stub; (b)Microstrip line phase shifter prototype (color online)

The four PIN diode phase shifters design is shown in Fig. 4, where D_{ij}, with i, j = {1, 2, 3, 4}, are PIN diodes with switch effect. Four bias voltage sources are used to control the states of the 16 PIN diodes in the phase shifters component.

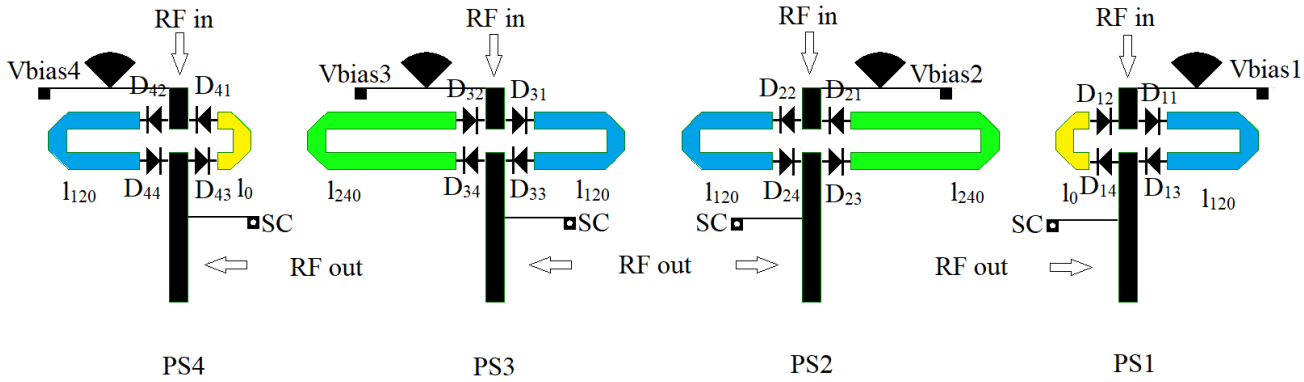

Fig. 4. Phase shifters design (color online)

The microstrip feed network design is an important factor in the antenna array design. In this paper, a corporate feed network is connected to phase shifters from Fig. 4. A 50 ohm microstrip transmission line, which splits into two, is used to excite the dielectric resonators of the array. So, in order to have a good matched feeding network, quarter-wave impedance transformers are used [9]. According to [10] the transmission lines are also mitered to minimize losses due to sharp corners.

Fig. 5 shows the geometric configuration of a corporate feed network for a four-element linear array antenna.

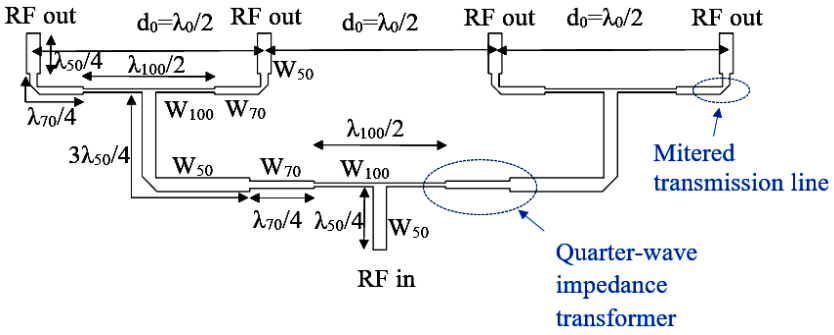

Fig. 5. A corporate feed network design for a four-element linear array antenna (color online)

where W_{50}, W_{70} and W_{100} are the width of microstrip lines of impedances 50 Ω, 70 Ω and 100 Ω, respectively, calculated with the formula from [7]. λ_{50}, λ_{70} and λ_{100} are the wavelengths corresponding to the microstrip lines of width W_{50}, W_{70} and W_{100}.

The geometric configuration of the corporate feed network connected to phase shifters for the proposed antenna array is shown in Fig. 6.

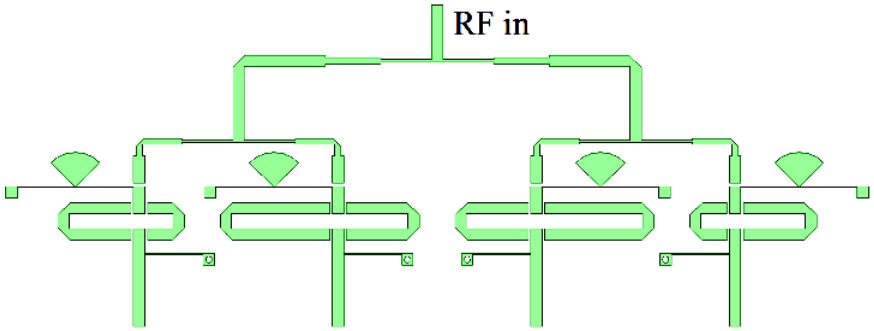

Fig. 6. A corporate feed network with PIN diode phase shifters for a four-element linear array antenna (color online)

Depending on the positive/negative states of the bias voltages, the signal is routed along paths of different lengths to obtain the desired phase shift. The bias voltages combinations to steer the antenna beam in a desired direction, are shown in Table 2.

Table 2. The bias voltages combinations to steer the antenna beam in a desired direction

Vbias1	Vbias2	Vbias3	Vbias4	Phase shift combination	Microstrip line combination			
					PS1	PS2	PS3	PS4
-	-	+	-	0º-240º-120º-0º	l_0	l_{240}	l_{120}	l_0
+	+	+	+	0º-0º-0º-0º	l_{120}	l_{120}	l_{120}	l_{120}
-	+	-	-	0º-120º-240º-0º	l_0	l_{120}	l_{240}	l_0

The equivalent circuits of a PIN diode in forward and reverse bias states are shown in Fig. 7.

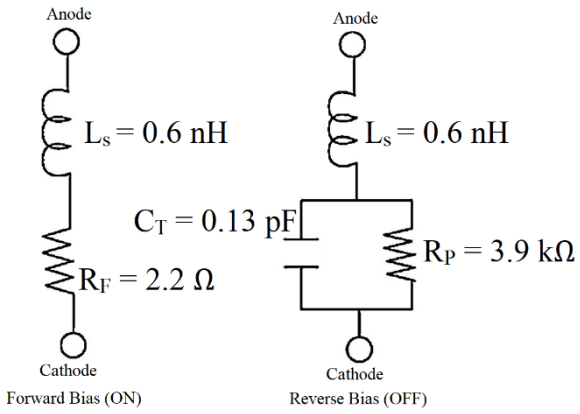

Fig. 7. The equivalent circuits for BAR64-02VPIN diode in forward and reverse bias states, at 1 GHz frequency

The antenna array has been tested for several PIN diode models, such as: BAR50-02V, BAR64-02V, BAR64-02EL, BAR90-02EL and BAR90-02ELS. The values was taken from technical data sheets of the producer [11]. Since, for certain frequencies, the R_F and C_T parameters of the diodes were not published in their data sheets, they were determined using [12].

Table 3. PIN diodes parameters

PIN diode	F [GHz]	I_f [mA]	V_R [V]	L_S [nH]	C_T [pF]	R_P [kΩ]	R_F [Ω]	I_L [dB]	I_{SO} [dB]
BAR50-02V	1.8	-	0	0.6	0.15	5	-	-	-
	1.8	10	-	0.6	-	-	3.16	0.27	-
	5.6	-	0	0.6	0.079	-	-	-	12
BAR64-02V	2.5	-	0	0.6	0.12	3	-	-	-
	2.5	10	-	0.6	-	-	2.4	-	-
	5.5	10	-	0.6	-	-	5.88	0.49	-
	5.5	-	0	0.6	0.138	-	-	-	7.7
BAR64-02EL	2.5	-	0	0.4	0.13	2.9	-	-	-
	2.5	10	-	0.4	-	-	2.5	-	-
	5.5	10	-	0.4	-	-	3.16	0.27	-
	5.5	-	0	0.4	0.136	-	-	-	7.8
BAR90-02EL	2.5	-	0	0.4	0.2	1.6	-	-	-
	2.5	10	-	0.4	-	-	1.7	-	-
	5.5	10	-	0.4	-	-	2.33	0.2	-
	5.5	-	0	0.4	0.189	-	-	-	5.6
BAR90-02ELS	2.5	-	0	0.2	0.16	1.5	-	-	-
	2.5	10	-	0.2	-	-	1.8	-	-
	5.5	10	-	0.2	-	-	1.63	0.14	-
	5.5	-	0	0.2	0.153				7

The simulations were performed using the High Frequency Structural Simulator (HFSS) from Ansys.

The antenna array reflection coefficient, corresponding to each PIN diode in Table 3, is plotted in Fig. 8.

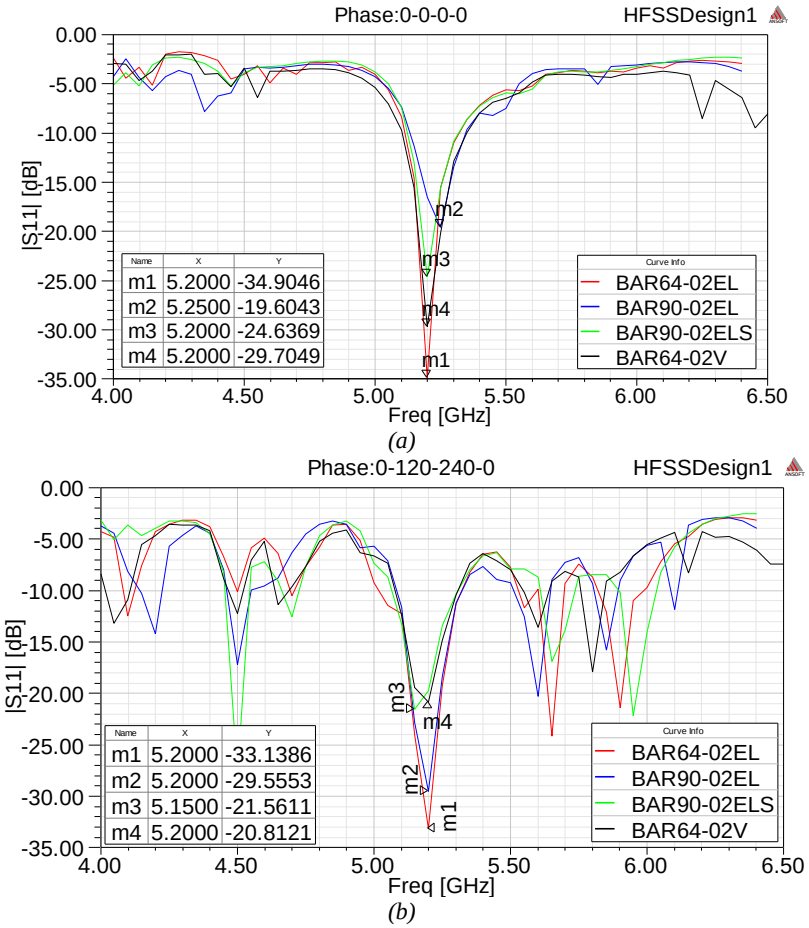

Fig. 8. Reflection coefficient |S11| for CDRA array with BAR64-02V, BAR64-02EL, BAR90-02EL and BAR90-02ELS PIN diodes. (a) Phase shift combination: 0º-0º-0º-0º. (b) Phase shift combination: 0º-120º-240º-0º (color online)

Analyzing the graphs in Fig. 8, it can be seen that, the reflection coefficient of the CDRA array has the best value, when the PIN BAR64-02EL diodes are used.

Using the previously mentioned diode, reflection coefficient, gain and radiation pattern of the CDRA array are plotted in Figs 9-11. The results are centralized in Table 4.

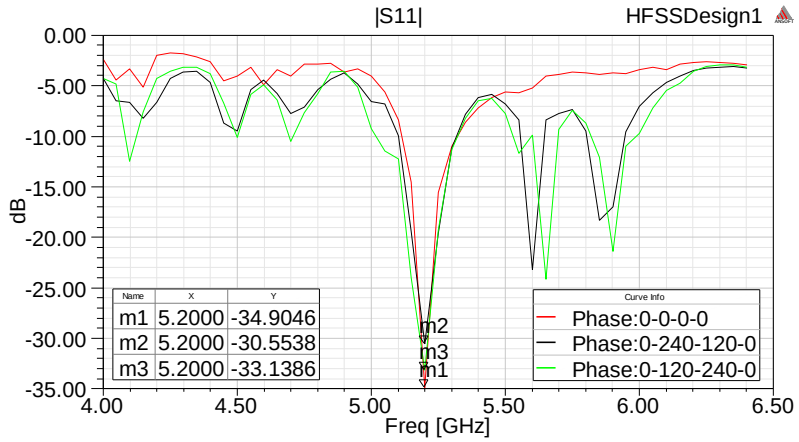

Fig. 9. Reflection coefficient |S11| of the antenna array depending on the combination of phases (color online)

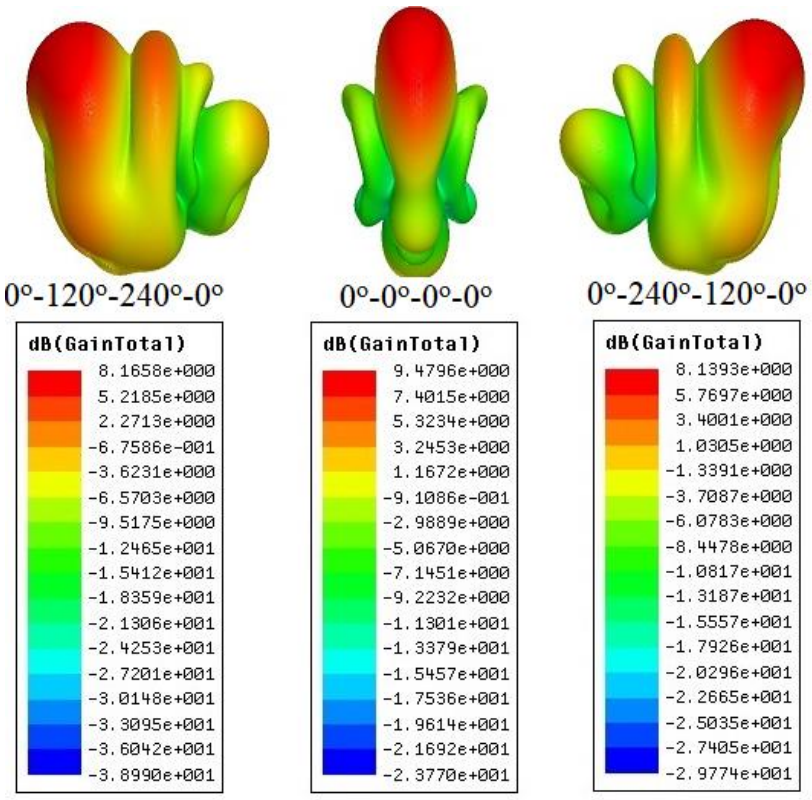

Fig. 10. Gain of the antenna array depending on the combination of phases (color online)

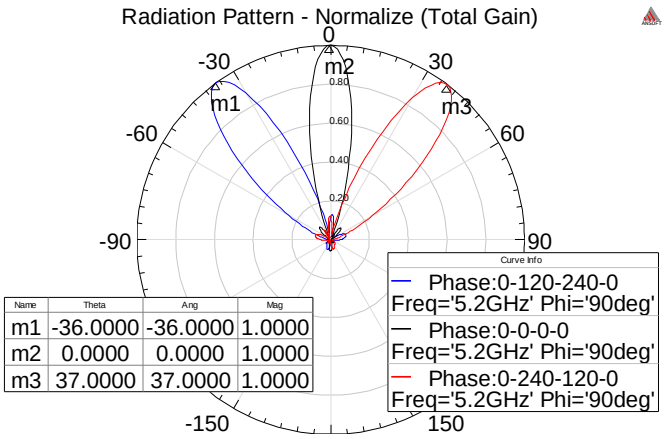

Fig. 11. Radiation pattern the antenna array depending on the combination of phases (color online)

The gain of the antenna array is 9.47 dB, when the signals applied to the array elements have the same amplitude and phase. The reflection coefficient is -34.90 dB, at resonant frequency of 5.2 GHz.

By performing a phase shift on the signals of the array elements, such 0º-120º-240º-0º, the resonant frequency doesn't changes. The situation is similar when we apply a phase shift like 0º-240º-120º-0º. In both cases, the antenna array is match to 50 Ω input impedance, the reflection coefficient being -33.13 dB and -30.55 dB, respectively.

The simulations showed that, depending on the combination of phases, the steering angles are: - 36, 0 and + 37 degree.

Table 4. Array parameters depending on the combination of phases

Phase shift	0º-120º-240º-0º	0º-0º-0º-0º	0º-240º-120º-0º
Steering angle (degree)	- 36	0	+ 37
f_0 (GHz)	5.2	5.2	5.2
|S11| (dB)	-33.13	-34.9	-30.55
-3 dB angle (degree)	29.27	23.88	28.86
-10 dB bandwidth (MHz)	303	207	217
VSWR	1.04	1.03	1.06
Gain (dB)	8.16	9.47	8.13
Difference between lobes (dB)	8.83	10.54	9.15
Radiation Efficiency (%)	66.97	73.20	65.73

3. Results

The proposed antenna array was practically implemented and the photograph of the prototype is shown in Fig. 12.

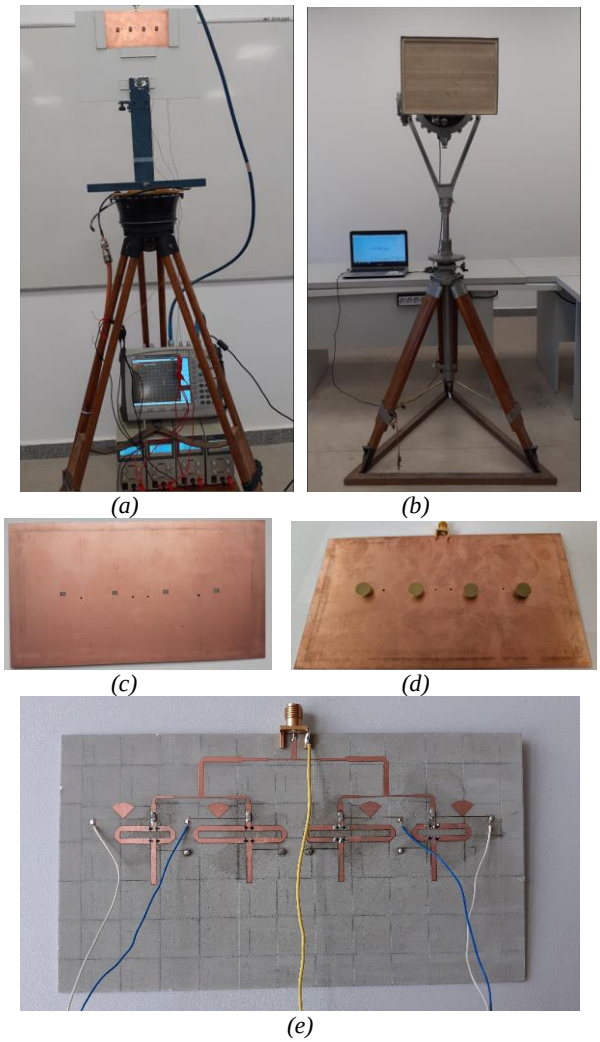

Fig. 12. A prototype of the fabricated antenna array. (a) The VNA connected to antenna array (b) The reference antenna horn connected to AVG POWER SENSOR NRP-Z221. (c) Top view with aperture. (d) Top view with CDRAs. (e) Bottom view (color online)

The reflection coefficient |S11| was measured using the Anritsu VNA MS2026C vector analyzer.

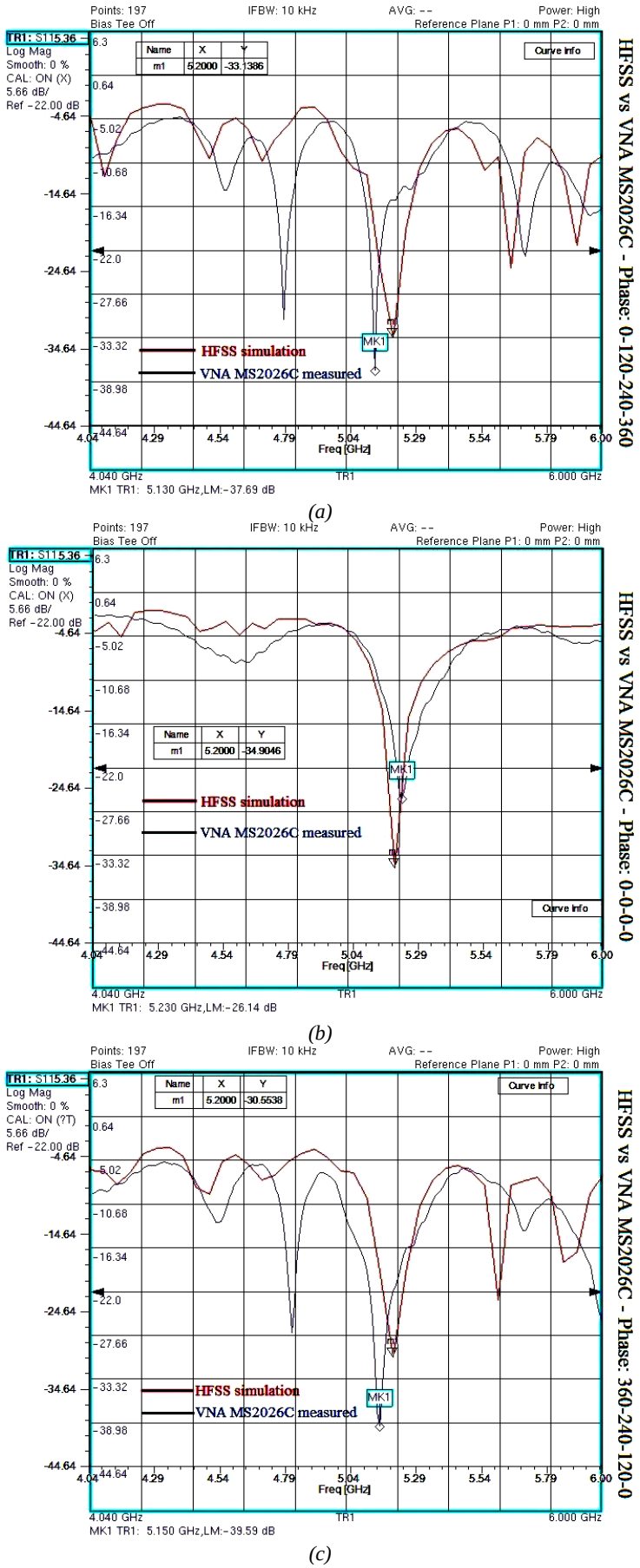

Fig. 13. Simulated vs. measured reflection coefficient |S11| for various cases (color online)

The amount of radiated energy around the antenna array was measured using the AVG POWER SENSOR NRP-Z221. The measured values were used to plot the antenna array radiation pattern.

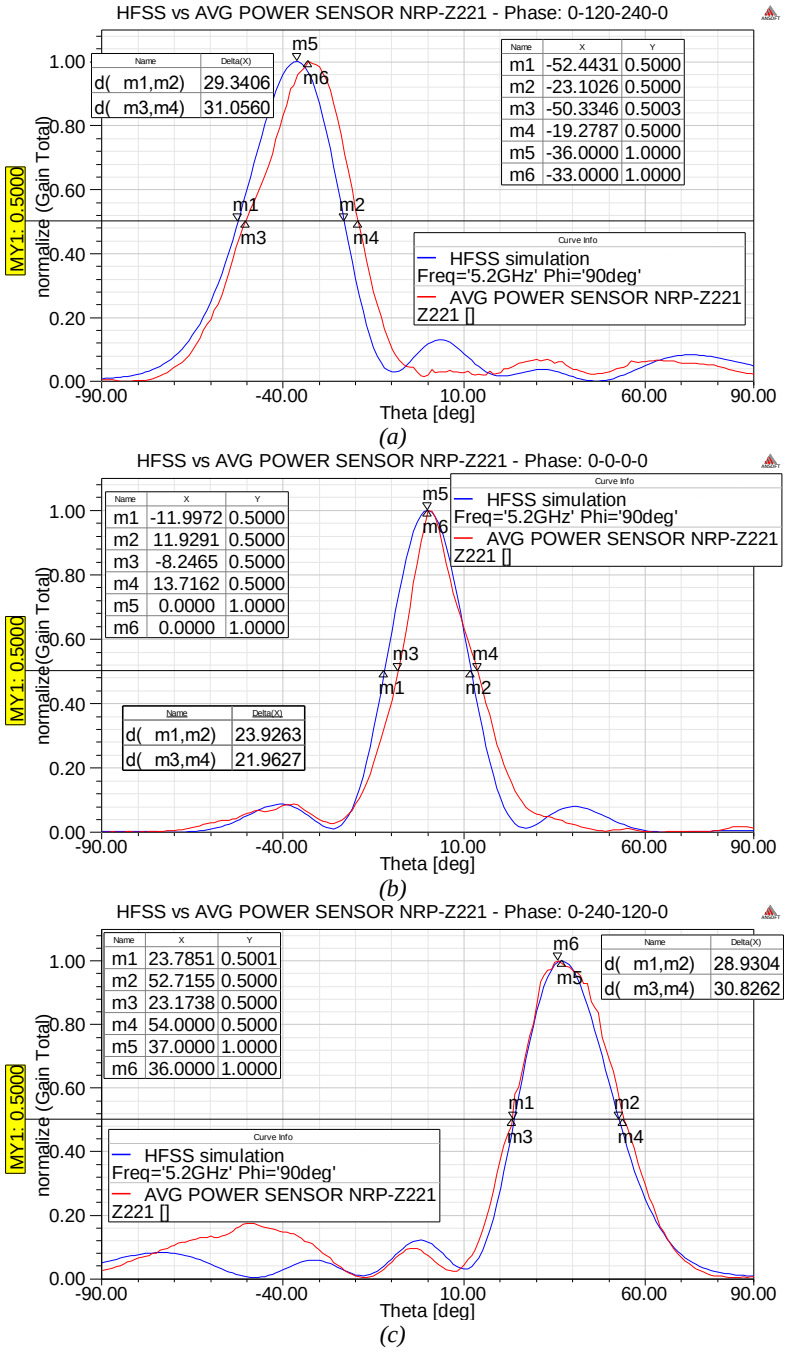

Fig. 14. Simulated vs. measured normalized radiation pattern (color online)

4. Discussions

The reflection coefficient for the antenna array is plotted in Fig. 13. For each case, the measured |S11| plot tends to have the same shape as the simulated |S11| plot. The deviations are minor, the resonance frequency changing from 5.2 GHz to: 5.23 GHz, for the phase shift 0º-0º-0º-0º, 5.13 GHz for the phase shift 0º-120º-240º-0º and 5.15 GHz for the last phase shift. The measured reflection coefficients, at the resonant frequency, for all cases are: -37.69 dB, -26.14 dB and -39.59 dB, which means a very good match of the antenna array to the 50 Ω input impedance.

As we expected, analyzing the graphs in Fig. 14, the measured radiation pattern is almost identical to the simulated one. The steering angles of the fabricated antenna array are: - 33, 0, and + 36 degree. The measure values for - 3 dB angle are 31.05, 21.96, 30.82 degree, which means that the fabricated antenna array is very directive.

The differences that occurred between simulated and measured values were due to several factors, such as:

- the excess material resulting from connecting the PIN diodes/capacitors to microstrip line;
- imperfect centering of the dielectric resonator over the slot;
- the glue used to fix the dielectric resonator to the ground plane [13];
- ovalization of the dielectric substrate, due to the manufacturing process of the corporate feed network;
- measuring antenna array parameters in an inadequate space.

Unfortunately, the radiation efficiency of the CDRA array is lower, around 73%, due to the insertion losses of the PIN diodes.

5. Conclusions

The phase shifters designed in this paper can be used to steer the main beam of an antenna array on different three directions.

A maximum beam steering angle of +36◦, with minimum reflection, and gain more than 8 dB, was obtained at the desired resonant frequency of 5.2 GHz.

To steer an antenna array beam in three directions, it is necessary to use a phase shifter with three states of phase shifts. In this work we used a phase shifter with two states of phase shifts. This was possible because, in 0^o-0^o-0^o-0^o phase shift combination case, each phase shifter used the l_{120} blue microstrip line, so that the signal reached to each antenna was of the same amplitude and phase.

Conventional open stubs can be successfully replaced by radial stubs. As observed, the length of an open stub can be reduced by up to 70 %, making the feed network much more compact.

The phase shifters have been designed small enough to fit on small structures so, the proposed antenna array has a compact size that, makes it an excellent candidate for small electronic devices.

The efficiency of the antenna array can be improved by using PIN diodes with low insertion loss and very high isolation. A very good candidate is the DSM8100-000 PIN diode. Unfortunately, the dimensions of these diodes are very small, their installation being possible only in specialized centers.

The proposed antenna array has a potential use in diverse applications, including automotive radar (to detect and locate obstacles in the surrounding environment, or in the mobile's vehicle blind spot area) and other beam steering technologies.

References

[1] Nipun K. Mishra, Soma Das, Cylindrical Dielectric Resonator Antenna Array with Beam Steering Capability, URSI AP-RASC 2019, New Delhi, India, 09 - 15 March 2019.
[2] L. P. Pontes, E. M. F. de Oliveira, C. P. N. Silva, A. G. Barboza, M. T. de Melo, Ignacio Llamas-Garro, Journal of Microwaves, Optoelectronics and Electromagnetic Applications **4**, 598 022).
[3] R. K. Mongia, P. Bhartia, International Jounal of Microwave and Millimeter-Wave Computer-Aided Engineering **4**(3), 230 (1994).
[4] J. C. Sethares, J. Naumann, IEEE Transactions on Microwave Theory and Techniques **14**(1), 2 (1966).
[5] Tang Xinyi, Broadband Phase Shifter Design for Phased Array Radar Systems, Dr. Phil. Thesis, National University of Singapore, 2011.
[6] F. R. Connor, Wave Transmission, Edward Arnold Ltd., 1972.
[7] T. R. Muthu, A. Thenmozhi, Optoelectron. Adv. Mat. **15**(5-6), 260 (2021).
[8] H. Atwater, Microwave Journal **28**(11), 149 (1985).
[9] Mohammad Tariqul Islam, Waled Yousef Noor Aboaresh, Dinh Nguyen Quoc, Rabah W. Aldhaheri, Khalid Hamed Alharbi, Abdulah Jeza Aljohani, MD Samsuzaman, J. Optoelectron. Adv. M. **22**(11-12), 564 (2020).
[10] R. J. P. Douville, D. S. James, IEEE Transactions on Microwave Theory and Techniques **26**(3), 175 (1978).
[11] https://www.infineon.com/cms/en/product/rf/rf-diode/rf-pin-diode/antenna-switch/;
[12] W. E. Doherty, R. D. Joos, The PIN Diode Circuit Designers Handbook, Watertown, MA: Microsemi Corp Print, 1 (1998).
[13] I. Nicolaescu, A. G. Avădanei, S. B. Balmuș, J. Optoelectron. Adv. M. **14**(11-12), 1005 (2012).

*Corresponding author: gabryel21@yahoo.com